# Preliminary analysis of a crosswell seismic dataset: Noel tight gas field, British Columbia

Joe Wong and Robert R. Stewart

## ABSTRACT

A crosswell seismic survey was acquired in the Noel oilfield, northeastern British Columbia, by Z-Seis Corporation for BP Canada Energy Company in 2004. The goal was to obtain data for high-resolution imaging of gas-bearing, but tight, sandstone channels about 2500 meters deep in the Cadomin and Nikanassin formations. Recording between two wells approximately 150 meters apart employed hydrophones and a piezoelectric vibrator source. Seismograms were produced post-acquisition by cross-correlating detected vibrations with the pilot sweeps. The dominant frequencies in the crosswell seismograms are about 500 to 1500 Hz, suggesting wavelengths on the order of 5 to 10 m. Compared to wavelengths of about 100 meters that are usual for surface seismic data, the shorter crosswell wavelengths provide significantly better resolution of beds 10 to 25 m thick. Preliminary processing of the data included sorting and display of gathers, band-pass filtering, and first-arrival time-picking. A P-wave velocity tomogram was created from observed first arrival times using an iterative back-projection algorithm and accounting for refracted arrival times in the low-velocity zones. Velocities were found to be in the range of 5800 to 6200 m/s for sandstone, and 5100 to 5500 m/s for the siltstones and shales. The seismic boundaries imaged in the tomogram correlate excellently with natural gamma ray logs and the known geology. Future analysis of the dataset will include migration of the up-going and down-going reflected events. In addition, we intend to investigate possible anisotropy in the strata along with attenuation. The velocity values will be compared to sonic logs and surface seismic analyses.

## INTRODUCTION

The Noel Gas Field, operated by BP Canada Energy Company, is located in northeastern British Columbia (Figure 1). Tight, gas-bearing sandstone channels exist at depths of 2400 to 2650 m in the Cadomin, lower Monach, and upper Monteith formations. Gas production from these target zones may be stimulated by hydraulic fracturing. Before deciding whether or not to go forward with a hydraulic fracturing program, BP Canada wished to have more detailed information regarding the continuity of the sand channels. To obtain this information, Z-Seis Corporation conducted a high-resolution crosswell seismic study between two wells, 00-A97-E and 02-A97-E, in June of 2004. BP Canada has generously provided the crosswell seismic records and other supporting data to the CREWES Project to use in its research efforts.

## INSTRUMENTATION AND ACQUISITION

The source used by Z-Seis Corporation was a piezoelectric vibrator controlled by a linear swept-frequency pilot signal. The sweep was 1.1 seconds long, beginning with a low frequency of 100 Hz and ending at a high frequency of 2000 Hz. The listen period was 1.6 seconds, and the digital sampling interval was 0.125 ms so that the Nyquist frequency was 4000 Hz. The sensors were an array of ten hydrophones separated by

1.5 meter intervals. Raw field data, i.e., the pilot signal and the received signals, were recorded for post-acquisition cross-correlation.
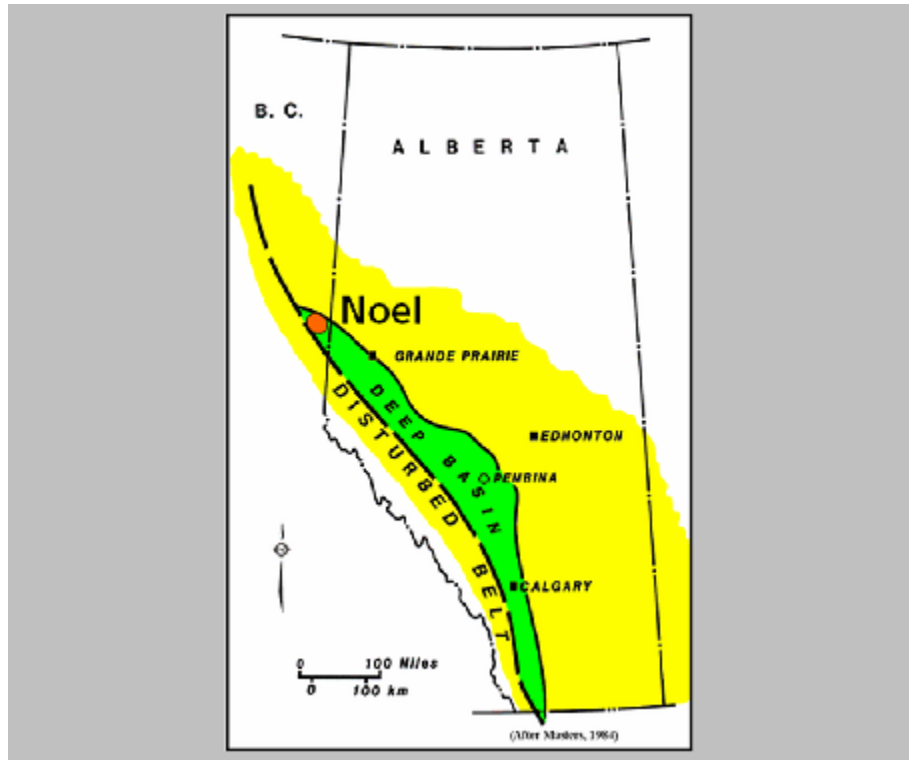
FIG. 1.  Location of the Noel Gas Field in northeastern British Columbia.

The following list is a summary of instrumentation and acquisition parameters.

- Piezoelectric source;
- Hydrophone receivers;
- Moving source: 10 m/minute;
- Source interval for recording = 0.75 m;
- Receiver spacing = 1.5 m;
- 1.1 second sweep, 100 to 2000 Hz;
- 1.6 second listen;
- 0.125 ms sampling.

Figure 2 shows a basic scanning pattern, with a source in one well transmitting into a number of receivers in a second well.  During field acquisition, the source was moved over a depth range of about 2300 to 2650 m at a speed of about 10 m per minute in 02-A97-E, while the hydrophone array was kept fixed in 00-A97-E.  Digital recording was timed so that a ten-channel record was stored at 0.75 m depth intervals for the source.  When coverage over the source depth range was complete, the receiver array was

moved to a new depth, and the process was repeated until the depth range of interest in the receiver well (2300 to 2650 m) was covered. This crosswell scanning procedure, with the source well sampled at 0.75 m depth intervals and the receiver well sampled at 1.5 m depth intervals, generated a dense network of over 59,000 unique raypaths crisscrossing the rock section between the two wells.
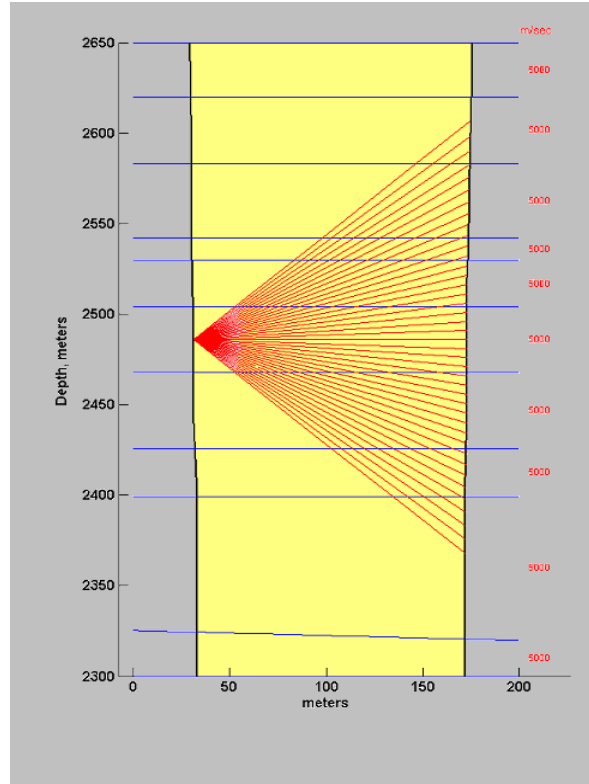


FIG. 2.  Schematic representation of crosswell seismic scanning.  A seismic source in the left-hand well sends seismic signals to receivers in the right-hand well.  A dense network of raypaths covering the rock section between is generated when the source and receivers occupy many depth locations.

## RAW FIELD RESULTS

The crosswell field records were provided to CREWES in uncorrelated form. Raw seismograms were generated by crosscorrelating the digitized hydrophone signals with the pilot signals. The seismograms were then sorted into various gathers for display and further analysis.  Figure 3a is a typical trace from the dataset, showing a very clear arrival. There appears to be some rippling before the first onset of seismic energy due to correlation noise. Figure 3b is the power spectrum of the trace, and it indicates that the significant frequencies in the received signals lie in the 100 to 2000 Hz range, identical to the range swept by the vibrator source.
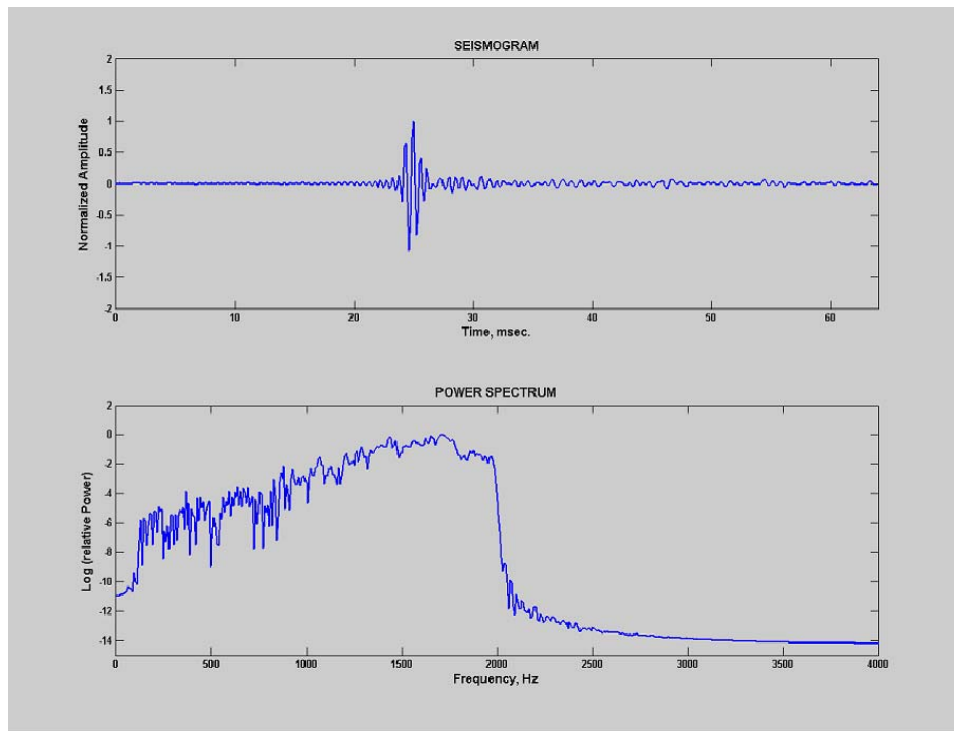
FIG. 3. (a) Top: a typical seismic trace from the Noel dataset. (b) Bottom: the normalized power spectrum. There is energy in the 100 to 2000 Hz frequency band, with a dominant frequency of about 1500 Hz.

The dominant frequencies in the crosswell seismograms are in the range 500 to 1500 Hz. Assuming P-wave velocities in the range 5000 to 6000 m/s, these frequencies suggest wavelengths on the order of 5 to 10 m. Compared to wavelengths of about 100 meters that are usual for surface seismic data, the shorter crosswell wavelengths should result in significantly better resolution of beds 10 to 25 m thick. The short wavelengths, coupled with the small depth intervals (0.75 m for the source, and 1.5 m for receivers) used in the survey, mean that this dataset has the potential of providing very detailed images of the structure between the two wells.

Figures 4a and 4b are typical common receiver gathers (not all traces on the gathers have been shown). Figure 4a is an AGC display in wiggle trace format. First arrivals stand very clearly above background noise levels near the apex of the gather. Decreases in signal strength on the flanks are due to geometric spreading and transmission/reflection effects at the seismic boundaries. Coherent events following the first arrivals are apparent, but the wiggle trace format is not the most effective display for emphasizing them. The variable-density, grey-scale format of Figure 4b brings out the fine details of a gather more effectively; coherent events following the first arrivals are visually much more prominent than they are on Figure 4a. The coherent events include up- and down-going reflections; these reflections will form the basis for future reflectivity imaging via VSP/CDP mapping (Wyatt and Wyatt, 1984; Li and Stewart, 1993; Lazaratos et al., 1995).
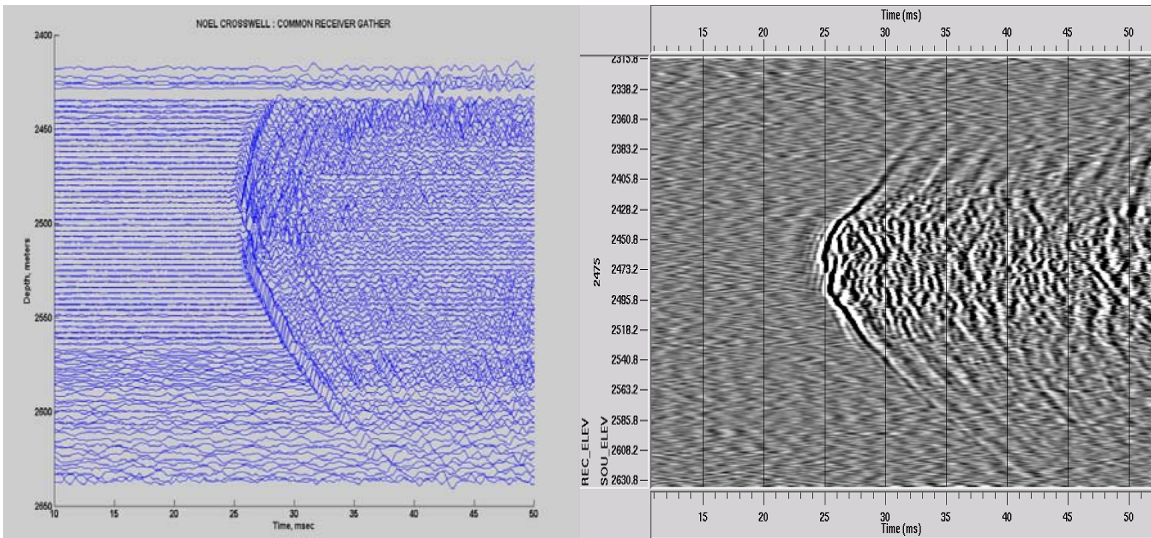
FIG. 4.  Two common receiver gathers: (a) wiggle trace display (left-hand side); (b) variable density display (right-hand side).  The variable density display shows the details of coherent events following the first arrivals more effectively.
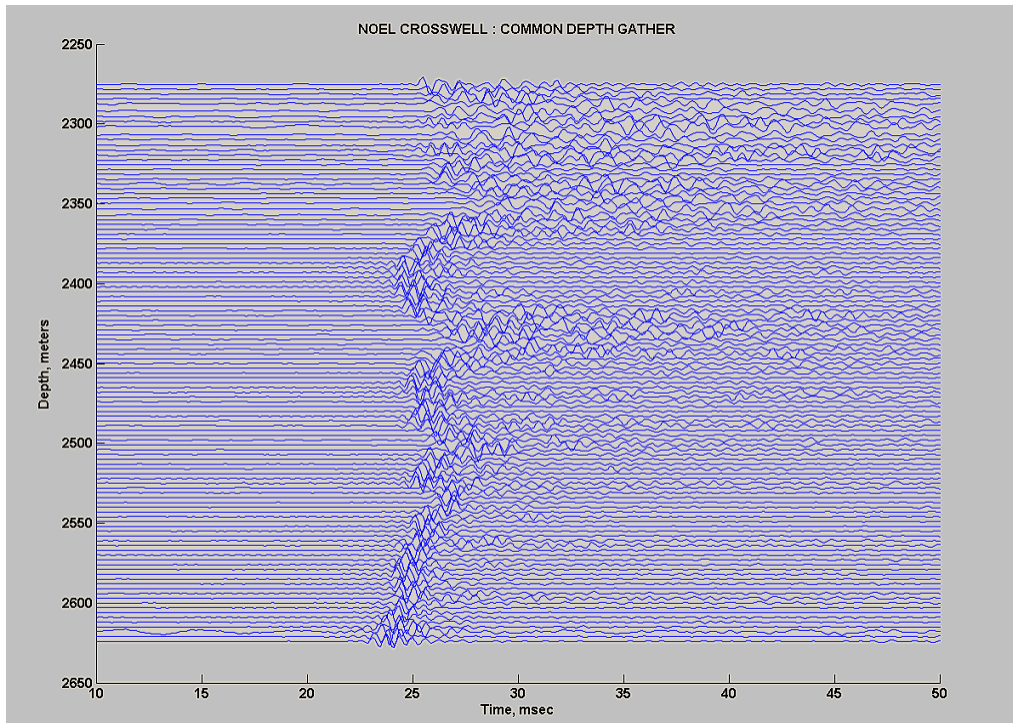


FIG. 5.  Common depth gather.  The first arrival times vary between 23 and 29 ms, reflecting the changing P-wave velocities of different lithological units.

## TIES TO GEOLOGY AND NATURAL GAMMA RAY LOGS

Figure 5 is a common depth gather that shows seismic traces having a near-horizontal travel path between the source and receiver wells. There are distinct variations with depth in the first onset times of seismic energy. These variations are due to the different P-wave velocities of the different lithological units.
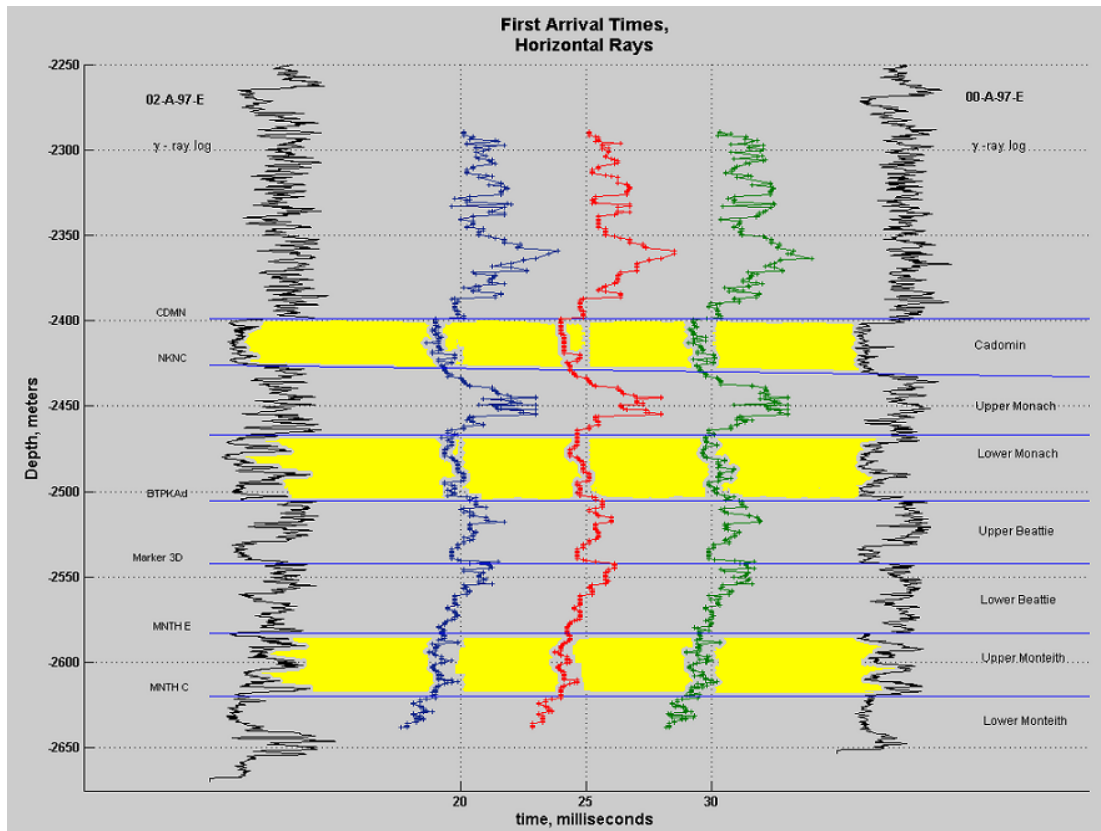


FIG. 6. Geology between the source well (02-A97-E) and the receiver well (00-A97-E), and the natural gamma-ray logs for the two wells. Also shown are three crosswell profiles for the zero-depth-offset first arrival times, each picked with slightly different criteria (red, green and blue curves). The time scale applies to the middle (red) profile. The tight, gas-bearing sandstone zones are high-lighted in yellow.

Figure 6 depicts the geological formations encountered by the two wells at the depth range of interest. The geology has a horizontally layered structure alternating between sandstones and siltstones/shales. The natural gamma-ray logs from the wells have been plotted on the sides of the figure. The sandstone target zones (i.e., the Cadomin, Upper Monach, and Lower Monteith formations) have been highlighted in yellow, and are associated with low responses on the natural gamma-ray logs. Non-gas-bearing shales and siltstones above and below the sandstone intervals are characterized by relatively higher gamma-ray activity.

We have picked the first arrival times for the common depth gathers automatically, using three slightly different criteria. These first arrival times have been plotted in Figure 6 between the natural gamma logs and on top of the geological units. There is good correlation between the common depth arrival times, the gamma-ray logs, and the

geological layering. Fast arrivals are associated with low gamma-ray activity and the sandstone formations, while slower arrivals are associated with higher gamma-ray responses and the siltstone/shale formations.

## VELOCITY TOMOGRAM

For the flat, horizontally-layered geology, the main features of the seismic velocity structure in the rock section are determined by the first arrival times of the common depth (or zero-offset) seismograms. An initial velocity tomogram was created by using first-arrival time picks from the zero-offset gather and gathers with source receiver depth-offsets of -50, -25, 25, and 50 m with a straight-ray, back-projection algorithm (Peterson et al., 1985; Wong et al., 1987).

The resulting first-pass P-wave velocity tomogram is shown in Figure 7a. While the major characteristics of the layered geology are present in the tomogram, the boundaries between layers are not as well-defined as might be desired. The decreased definition of the boundaries is due to strictly using first arrival times in producing the tomogram. In a low-velocity layer at locations close to the boundaries separating it from the higher-velocity zones above and below it, first arrival times will be from raypaths which follow refracted trajectories that go through the higher-velocity zones for much of their trajectories. The corresponding arrival times are faster than if the paths had remained entirely within the low-velocity formations. When the arrival times from these refracted rays are used in tomogram creation without consideration for this "speed-up" behavior, we produce a bias toward higher velocity values in the low-velocity zones. This bias causes a loss of contrast with the higher velocity zones above and below.

We can eliminate the bias and improve the contrast if, instead of using the first arrival times strictly, we identify the low-velocity zones (using the first-pass tomogram, natural gamma-ray logs, and the geology intersected by the wells) and make corrections to the zero-offset arrival times before a creating second-pass image. The corrections to the zero-offset arrival times through low-velocity zones are made in a way that is consistent with refraction into and out of the high-velocity zones above and below. A tomogram created with the corrected arrival times will then (1) account for refraction; (2) correlate better with known geology; (3) define geological boundaries more sharply; and (4) have more accurate velocity values.

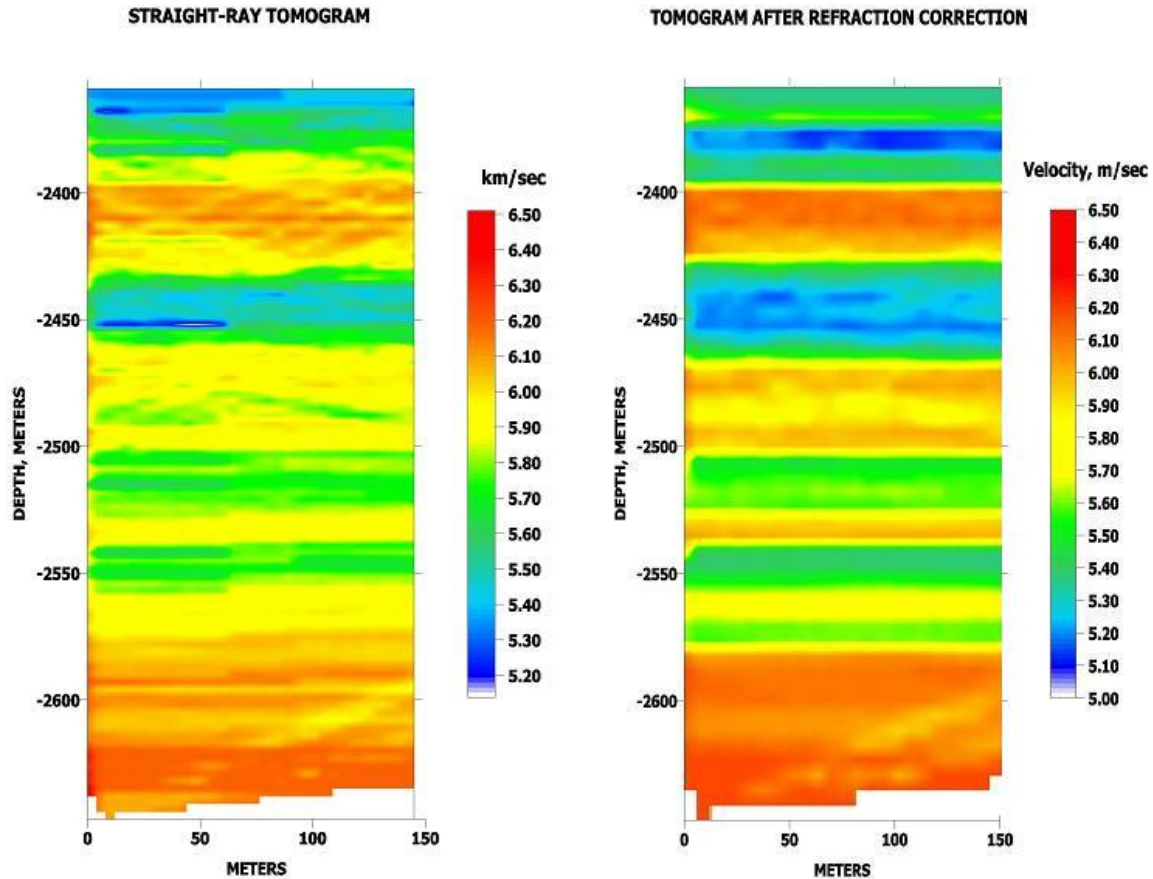STRAIGHT-RAY TOMOGRAM           TOMOGRAM AFTER REFRACTION CORRECTION



FIG. 7. P-wave velocity tomograms. (a) First-pass tomogram, created by back-projection of raw first arrival times. (b) Second-pass tomogram, created after correction to zero-offset arrival times in low-velocity zones for refraction into and out of adjacent high-velocity strata.

This has been done, and the resulting second-pass tomogram is shown in Figure 7b. The boundaries between formation units are sharper than those in Figure 7a. The second-pass tomogram is displayed in Figure 8 overlaid on the known geology, with the natural gamma-ray logs plotted on either side. The correspondence of the velocity structure as depicted by the tomogram with the geological layers and the gamma-ray logs is excellent. In general, the sandstones are associated with higher velocity values while the siltstones/shales are associated with lower velocity values. The sandstone in the Cadomin, the Lower Monach, and the Upper Monteith formations have P-wave velocities in the range 5800 to 6200 m/s, while the siltstones and shales of the other geological units have velocities of 5100 to 5500 m/s.

It should be noted that the velocity tomograms were created assuming that the well-to-well separation was 150 m with no depth variation. We made this assumption because hole deviation surveys were not available for us to map the well trajectories. We hope to obtain the deviation information and the sonic logs for the source and receiver wells in the near future. We anticipate that, by using more accurate well trajectories and sonic logs as velocity constraints with the tomographic reconstruction process, we will obtain a more accurate P-wave velocity model.
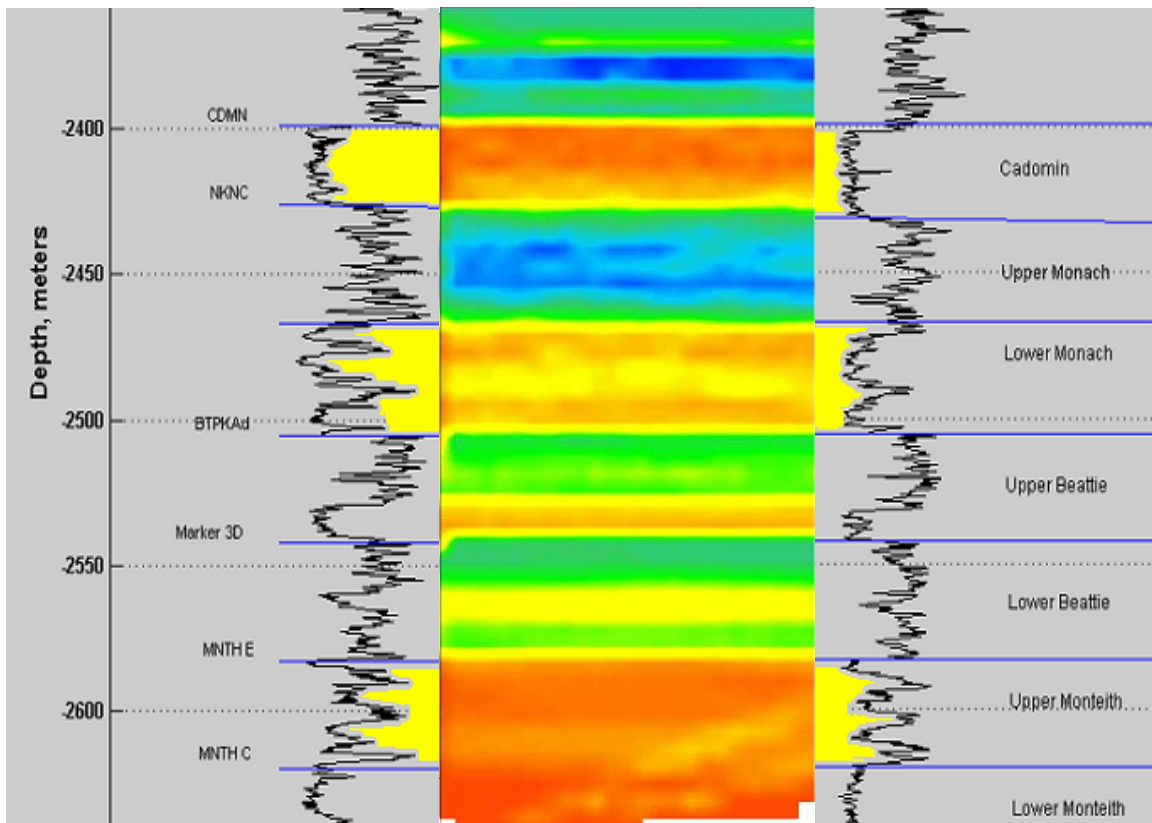
FIG. 8.  P-wave velocity tomogram overlain on Figure 6.

## CONCLUSIONS

A crosswell seismic survey carried out in 2004 by Z-Seis Corporation for BP Canada Energy Company produced a very detailed, high-quality dataset for studying the continuity of tight, gas-bearing sand channels in the Cadomin, Lower Monach, and Upper Monteith formations in the Noel Gas Reservoir in northeastern British Columbia. CREWES was given the opportunity to analyze the data, and initial results have been given in this report.

The seismic survey was carried out with a swept-frequency piezoelectric source in well 02-A97-E and an array of 10 hydrophones in well 00-A97-E.  The linear sweep used was 1.1 seconds long, with a start frequency of 100 Hz and an end frequency of 2000 Hz. The listen period was 1.6 seconds, and the sampling interval during was 0.125 ms. Crosswell scanning was conducted with 0.75 m depth intervals in the source well and 1.5 meters in the receiver well, resulting in a very dense network of more than 59,000 raypaths in the rock section between the wells.

Crosscorrelation of the raw received signals with swept-frequency pilot controlling the source yielded the seismic traces.  The seismograms were sorted into common receiver and common depth gathers for display and for first arrival time-picking.   Zero-depth-offset first arrival times correlate well with the known geology and natural gamma logs in

the source and receiver wells. A P-wave velocity tomogram, created from first-arrival travel times corrected for turning-ray refraction out of and back into low-velocity zones, clearly delineates the sandstones, siltstones, and shales. Velocity values are in the range 5800 to 6200 m/s for the sandstones and 5100 to 5500 m/s for the siltstones and shales. However, because we did not have accurate well deviation surveys, these values are based on an assumed well-to-well separation of 150 m, and likely will change when more accurate well trajectories become available and used as input for tomogram construction.

## FUTURE WORK

Analysis of the Noel crosswell dataset will proceed beyond the results in the present report. Improvements in the velocity tomogram require the inclusion of well deviation information and sonic logs, and the use of curved rays in the modeling of arrival times. Improvements are necessary since we need as accurate as possible a velocity model for the next major step in analysis, namely, reflectivity imaging.

In the raw data, we see many coherent reflections that originate at the geological boundaries. By filtering out direct arrivals and tube waves, we will isolate these up- and down-going reflected wavefields. Reflectivity imaging via VSP/CDP mapping of both wavefields will provide an alternate picture of the geological section between the wells. Because of tight sampling in depth (source intervals of 0.75 m; receiver intervals of 1.5 m) and high frequencies, the potential for resolving features with sizes on the order of 3 to 5 meters is excellent.

## ACKNOWLEDGEMENTS

## REFERENCES

Lazaratos, S.K., Harris, J.M., Rector, J.W., and Van Schaak, M., 1995, High-resolution crosswell imaging of a west Texas carbonate reservoir: Part 4 – Reflection imaging: Geophysics, **60**, 702-711.

Li, G., and Stewart, R.R., 1993, Reflection imaging for crosswell seismic data: Friendswood, Texas: CREWES Research Report, **5**, 5b.1-5b.28.

Peterson, J.E., Paulsson, J.N.P., and McEvilly, T.V., 1985, Application of algebraic reconstruction techniques to crosswell seismic data: Geophysics, **50**, 1566-1580.

Wong, J., Bregman, N., Hurley, P., and West, G.F., 1987, Crosshole seismic tomography: The Leading Edge, **6**, 36-41.

Wyatt, K.D., and Wyatt, S.B., 1984, Determining subsurface structure using the vertical seismic profile, *in*, Toksoz, M.N., and Stewart, R.R., Eds., Vertical Seismic Profiling, Part B: Advanced Concepts, Geophysical Press, 148-176.